Comparison Between Phase Unwrapping Algorithms for Depth Estimation in 1-D Wavelet Profilometry

Jesus Carlos Pedraza-Ortega[1], Efren Gorrostieta-Hurtado[1], Emilio Vargas-Soto[1], Juan Manuel Ramos-Arreguín[1], Marco Aceves-Fernández[1], Carlos Alberto Olmos-Trejo[1], Sandra Luz Canchola-Magdaleno1, Saúl Tovar-Arriaga[1], Artemio Sotomayor-Olmedo[1],

[1] UAQ, Facultad de Informática, Querétaro, México.
carlos.pedraza@uaq.mx, efrengorrostieta@gmail.com, emilio@mecatronica.net, juan.ramos@uaq.mx, marco.aceves@uaq.mx, caolmos@uaq.mx, sandra.canchola@uaq.mx , saulotovar@hotmail.com, artemio.sotomayor@uaq.mx

Abstract. Transform based profilometry has been widely used for three-dimensional (3-D) surface shape measurement using a projected fringe pattern. These methods require a single image with a sinusoidal fringe pattern projected on it. The projected pattern has a known spatial frequency and its information is used to avoid any discontinuities in the fringes with high frequency. Among single projected fringe pattern, most of the methods use Fourier or Wavelet transforms to extract the phase information. However, they focused only on the transform method and not on the phase unwrapping algorithms. In this paper, a 1-D wavelet profilometry method is presented considering two different wavelet transforms. Later, different phase unwrapping algorithms are used to extract the depth information considering local and global analysis. Several computer simulations and experiments are carried out to validate the proposed method. The merits and limitations of each of these variations on the method are indicated and the error is estimated.

Keywords: Phase unwrapping; depth estimation; algorithms; wavelet transform

1 Background

In order to extract the 3D information of an object, several contact and non-contact measurement techniques have been employed. The main idea is to extract the useful depth information from an image or set of images in an efficient and automatic way. The result of the process (depth information) can be used to guide various tasks such as synthetic aperture radar (SAR), magnetic resonance imaging (MRI), automatic inspection, reverse engineering, 3D robot navigation, interferometry and so on [1]. The contact measurement techniques provide a better way to realize this process by using a vision system together with a tool in contact with the object, like laser, fringe projection and so on. Among all the diverse techniques, one of the most widely used is the fringe projection. Fringe processing methods are widely used in non-destructive testing, optical metrology and 3D reconstruction systems. Some of the desired characteristics in these methods are high accuracy, noise-immunity and fast

Advances in Computer Science and Electronic Systems
Research in Computing Science 52, 2011, pp. 190-203
Received 23/01/11
Accepted 20/02/11
Final version 07/03/11

processing speed. The most known fringe processing methods are the Fourier Transform Profilometry (FTP) method [2], Phase-shifting or phase stepping [3, 4], digital phase locked loop [5], direct phase detection [6], and Wavelet Transform Profilometry [12, 16]. Among all the methods, one of the main challenges is the problem of wrapped phase information problem due to the fact that the phase of a periodically varying intensity pattern is encoded or wrapped and it contains the depth information of the object. The phase unwrapping problem has been attacked by several researchers who have attempted to solve it in many ways. Historically, one of the first algorithms to deal with this problem was proposed by Takeda and Mutoh in 1982 [2]. Later Berryman [7] and Pedraza [8, 17, 18] proposed a modified Fourier Transform Profilometry by carrying out global and local analyses in the phase unwrapping step. Then, unwrapping algorithms (temporal and spatial) were introduced and modified [7-10]. Phase unwrapping techniques use exhaustive data computations and approximations, however, these approaches have a small contribution to understand the cause of failure in the phase unwrapping process. This research presents an implementation of phase unwrapping algorithms, considering the problem of residues.

Generally, most of the proposed methods used a Fourier Transform Profilometry, and another suitable solution is to use the wavelet transform extract the information.

Wavelet transform offers multi-resolution in time and space frequency, and it is a tool that offers advantages over the Fourier transform [9-10]. The computation in the method can be carried out by analyzing the projected fringe patterns using a wavelet transform. Mainly, this analysis consists of demodulating the deformed fringe patterns and extracting the phase information encoded into it and hence the height profile of the object can be calculated, quite similar to Fourier transform.

Different wavelet algorithms are used in the demodulation process to extract the phase of the deformed fringe patterns. Those algorithms can be classified into two categories: phase estimation and frequency estimation techniques. The phase estimation algorithm employs complex mother wavelets, here, the extracted phase suffers from 2π discontinuities and a phase unwrapping algorithm is required to remove these 2π jumps. Zhong et al. [9] have applied Gabor wavelets to extract the phase distribution where a phase unwrapping algorithm is required. The frequency estimation technique estimates the instantaneous frequencies in a fringe pattern, which are then integrated to estimate the phase. The phase extracted using this technique is continuous; consequently, phase unwrapping algorithms are not required for 2D Wavelet Profilometry. Complex or real mother wavelets can be used to estimate the instantaneous frequencies in the fringe pattern. Dursun et al. [14] and Afifi et al. [15] have used Morlet or Paul wavelets, separately, to obtain the phase distribution of projected fringes. Also, Gdeisat et al. [16] have proposed a 1D continuous wavelet transform approach to retrieve phase information in temporally and spatially fringe patterns.

Most of the previous research is focused on using the Fourier and wavelet transforms to obtain the 3D information from an object; pre-filtering the images, extracting the phase information of fringe patterns, using phase unwrapping algorithms, and so on.

In the present research, a comparison between two phase unwrapping algorithms is presented in 1D Wavelet Profilometry is presented in order to obtain the 3D information from an object. First, the spatial frequency of the projected fringe pattern

is obtained; later the mathematical model is obtained and used together with the spatial frequency in order to establish the problem. Then, a 1D Wavelet Profilometry is applied considering the most suitable wavelets for the analysis. Later, three phase unwrapping algorithms are used to obtain the desired 3D information. One contribution of this research is the proposed methodology, because in previous works there are no comparison among different phase unwrapping (PU) methods in 1D Wavelet based profilometry. The results show that it's suitable to compare the present work with other similar researches. To test the method, some virtual objects were created for use in computer simulations and also some experiments were carried out.

2 Profilometry Basics

As described early, there are several fringe projection techniques which are used to extract the three-dimensional information from the objects. The two mostly used techniques (Fourier Transform and Wavelet Profilometry) are presented.

2.1 Fourier Transform Profilometry (FTP)

The image of a projected fringe pattern and an object with projected fringes on it, as shown on figure 3, can be represented by:

$$g(x,y) = a(x,y) + b(x,y) * \cos[2 * \pi f_0 x + \varphi(x,y)] \quad (1)$$

$$g_0(x,y) = a(x,y) + b(x,y) * \cos[2 * \pi f_0 x + \varphi_0(x,y)] \quad (2)$$

where $g(x,y)$ and $g_0(x,y)$ are the intensities of the images at the point (x,y), $a(x,y)$ represents the background illumination, $b(x,y)$ is the contrast between the light and dark fringes, f_0 is the spatial-carrier frequency and $\varphi(x,y)$ and $\varphi_0(x,y)$ are the corresponding phase to the fringe and distorted fringe pattern.

The phase $\varphi(x,y)$ contains the desired information. This angle $\varphi(x,y)$ is the phase shift caused by the object surface end the angle of projection, and its expressed as:

$$\varphi(x,y) = \varphi_0(x,y) + \varphi_z(x,y) \quad (3)$$

where $\varphi_0(x,y)$ is the reference plane projected phase angle, and $\varphi_z(x,y)$ is the object's height distribution phase.

In Pedraza et al work [17, 18], the Equation 5 can be rewritten as:

$$\varphi_z(x,y) = \frac{h(x,y)2\pi f_0 d_0}{h(x,y) - l_0} \quad ; h(x,y) = \frac{l_0 \phi_z(x,y)}{\phi_z(x,y) - 2\pi f_0 d_0} \quad (4)$$

where the value of $h(x,y)$ is measured and considered as positive to the left side of the reference plane. Also, the Equation 4 expresses the height distribution as a function of the phase distribution.

The Equation 1 can be rewritten as:

$$g(x,y) = \sum_{n=-\infty}^{\infty} A_n r(x,y) \exp(in\varphi(x,y)) * \exp(i2\pi n f_0 x) \quad (5)$$

where r(x,y) is the reflectivity distribution on the diffuse object [3,4]. Then, a FFT (Fast Fourier Transform) is applied to the signal in the x direction only. Thus, the following equation is obtained:

$$G(f,y)=\sum_{-\infty}^{\infty}Q_n(f-nf_0,y) \tag{6}$$

where Q_n is the 1D Fourier Transform of $An\ exp[in\varphi(x,y)]$.

Here $\varphi(x,y)$ and $r(x,y)$ vary very slowly in comparison with the fringe spacing, then the Q peaks in the spectrum are separated from each other. It is also necessary to consider that if a high spatial fringe pattern is chosen, the FFT will have a wider spacing among the frequencies; this behavior helps to identify the fundamental peak f_0. In FTP, next step is to remove all signals but positive fundamental peak f_0. Then, the result is shifted and centered. Later, the IFFT (Inverse Fast Fourier Transform) is applied in the x direction only. Here, is necessary to separate the phase part of the result from the rest because it contains the depth information:

$$\begin{aligned}\varphi_z(x,y)&=\varphi(x,y)+\varphi_0(x,y)\\&=\mathrm{Im}\{\log(\hat{g}(x,y)\hat{g}_0^{*}(x,y))\}\end{aligned} \tag{7}$$

The whole phase map is obtained by applying the same procedure for each x line. The result is that the values of the phase map are wrapped at some specific values whose range lie between π and $-\pi$. Then, to recover the true phase it is necessary to restore the measured wrapped phase by an unknown multiple of $2\pi f_0$ [17]. However, to analyze and describe signals, it requires information from both domains time and frequency, therefore Fourier is not a suitable solution to express those signals and another way is proposed, wavelet transform.

2.2 Wavelet Transform Profilometry

The wavelet transform (WT) is considered an appropriate tool to analyze non-stationary signals. This technique has been developed as an alternative approach to the most common transforms, such as Fourier transform, to analyze fringe patterns. Furthermore, WT has a multi-resolution property in both time and frequency domains which solves a commonly know problem in other transforms like the resolution.

A wavelet is a small wave of limited duration (this can be real or complex). For this, two conditions must be satisfied: firstly, it must have a finite energy. Secondly, the wavelet must have an average value of zero (admissibility condition). It is worth noting that many different types of mother wavelets are available for phase evaluation applications. The most suitable mother wavelet is probably the complex Morlet one [2]. The Morlet wavelet is a plane wave modulated by a Gaussian function, and is defined as:

$$\psi(x)=\pi^{1/4}\exp(icx)\exp(-x^2/2) \tag{8}$$

where c is a fixed spatial frequency, and chosen to be about 5 or 6 to satisfy an admissibility condition [11]. Figure 1 shows the real part (dashed line) and the imaginary part (solid line) of the Morlet wavelet.

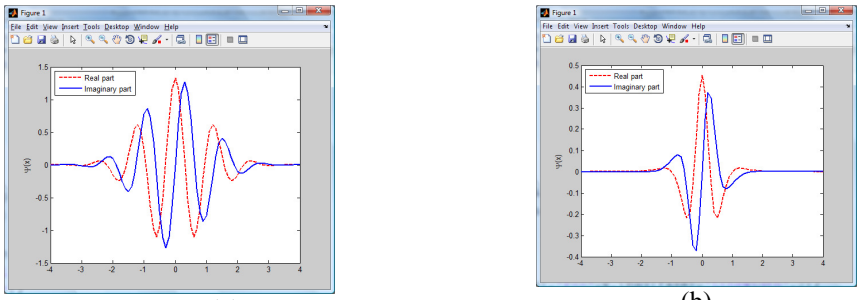

Figure 1. Mother Wavelets: (a) Complex Morlet and (b) Paul.

Also, Paul Wavelet is considered as one choice to perform the phase evaluation and is defined as:

$$\psi(x) = \frac{2^n n!(1-ix)^{-(n+1)}}{2\pi\sqrt{\frac{(2n)!}{2}}} \tag{9}$$

where n is the order of the Paul mother wavelet and chosen to have the value of 5.

The one-dimensional continuous wavelet transform (1D-CWT) of a row $f(x)$ of a fringe pattern is obtained by translation on the x axis by b (with y fixed) and dilation by s of the mother wavelet $\psi(x)$ as given by:

$$W(s,b) = \frac{1}{\sqrt{s}} \int_{-\infty}^{\infty} f(x)\psi^*\left(\frac{x-b}{s}\right)dx \tag{10}$$

here, * denotes complex conjugation and $W(s,b)$ is the calculated CWT coefficients which refers to the closeness of the signal to the wavelet at a particular scale.

In this research, the phase estimation and frequency estimation methods are used to extract the phase distribution from two dimensional fringe patterns. In the phase estimation method, a complex Morlet and Paul wavelets will be applied to a row of the fringe pattern. The resultant wavelet transform is a two dimensional complex array, where the phase arrays can be calculated as follows:

$$abs(s,b) = |W(s,b)| \tag{11}$$

$$\varphi(s,b) = \tan^{-1}\left(\frac{\Im\{W(s,b)\}}{\Re\{W(s,b)\}}\right) \tag{12}$$

To compute the phase of the row, the maximum value of each column of the modulus array is determined and then its corresponding phase value is found from the phase array. By repeating this process on all rows of the fringe pattern, a wrapped phase map results and an unwrapping algorithm is then needed to unwrap it.

In the frequency estimation method, a complex Morlet wavelet and Paul wavelet are applied to a row of the fringe pattern. The resultant wavelet transform is a two dimensional complex array. The modulus array can be found using Equation (14) and hence the maximum value for each column and its corresponding scale value can be determined. Considering that we are interested in the 1D signal:

$$f(x) = a(x) + b(x)\cos(2\pi f_0 x + \varphi(x)) \tag{13}$$

Considering the Euler identity for cos(x), we can re-write the Equation 13 as:

$$f(x) = a(x) + b(x)\cos(\varphi(x)) = a(x) + b(x)\frac{e^{i\varphi(x)}}{2} + b(x)\frac{e^{-i\varphi(x)}}{2} \tag{14}$$

The analytic function *f* in an open interval A, where $z_0 \in A$ can be decomposed into Taylor series:

$$f(z) = \sum_{k=0}^{\infty} \frac{f^{(k)}(z_0)}{k!}(z - z_0)^k \tag{15}$$

Therefore:

$$\varphi(x) = \varphi(x) + \varphi'(x)(b)(x-b) + \frac{\varphi''(x)}{2!}(x-b)^2 + \frac{\varphi'''(x)}{3!}(x-b)^3 + \ldots \tag{16}$$

If :

$$\varphi(x) = \varphi(b) + \varphi''(b) \approx 0,\ \varphi'''(b) \approx 0,\ \varphi'^{v}(b) \approx 0, \cdots, \varphi^k(b) \approx 0 \tag{17}$$

Then, the function can be reduced as:

$$\varphi(x) = \varphi(b) + \varphi'(b)(x-b) \tag{18}$$

Moreover, the Morlet Wavelet is defined as $\psi(x) = e^{i\varpi_0 x}e^{-\frac{x^2}{2}}$, this wavelet will be applied to the mother wavelet $W(s,b) = \frac{1}{s}\int_{-\infty}^{\infty} f(x)\psi^*\left(\frac{x-b}{s}\right)dx$:

If s = 1, then:

$$\begin{aligned} W(s,b) &= \frac{1}{s}\int_{-\infty}^{\infty} f(x)\psi^*\left(\frac{x-b}{s}\right)dx \\ &= \int_{-\infty}^{\infty}\left[a(x) + b(x)\frac{e^{i\varphi(x)}}{2} + b(x)\frac{e^{-i\varphi(x)}}{2}\right]\psi^*\left(\frac{x-b}{s}\right)dx \\ &= a\int_{-\infty}^{\infty}\psi^*\left(\frac{x-b}{s}\right)dx + \frac{b}{2}\int_{-\infty}^{\infty}\frac{e^{i[\varphi(b)+\varphi'(b)(x-b)]}}{2}\psi^*\left(\frac{x-b}{s}\right)dx + \frac{b}{2}\int_{-\infty}^{\infty}\frac{e^{-i[\varphi(b)+\varphi'(b)(x-b)]}}{2}\psi^*\left(\frac{x-b}{s}\right)dx \end{aligned} \tag{19}$$

By solving Equation 19, the following equation is obtained:

$$a\sqrt{2\pi}e^{-\frac{1}{2}\varpi_0^2} + \frac{b}{2}\sqrt{2\pi}e^{-\frac{1}{2}(\varpi_0 + s\varpi_s)^2}e^{-i\varpi_s b} + \frac{b}{2}\sqrt{2\pi}e^{-\frac{1}{2}(\varpi_0 - s\varpi_s)^2}e^{i\varpi_s b} \tag{20}$$

Then the instantaneous frequencies are computed using the next Equation [11]:

$$\hat{f}(b) = \frac{c + \sqrt{c^2+2}}{2s_{\max}(b)} - 2\pi f_o \tag{21}$$

where f_0 is the spatial frequency. At the end, the phase distribution can be extracted by integrating the estimated frequencies.

The same procedure can be developed to get the instantaneous frequencies, which lead us to have the wrapped phase and therefore it is necessary to apply a phase unwrapping algorithm.

3 Phase Unwrapping

Since two decades ago, phase unwrapping has been a research area and many papers have been published, presenting some ideas that solves the problem. Several phase unwrapping algorithms have been proposed, implemented and tested.

The phase unwrapping process is not a trivial problem due to the presence of phase singularities (points in 2D, and lines in 3D) generated by local or global undersampling. The correct 2D branch cut lines and 3D branch cut surfaces should be placed where the gradient of the original phase distribution exceeded π rad value. However, this important information is lost due to undersampling and cannot be recovered from the sampled wrapped phase distribution alone. Also, is important to notice that finding a proper surface, or obtaining a minimal area or using a gradient on a wrapped phase will not work and one could not find the correct branch in cut surfaces.

The phase unwrapping has many applications in applied optics that require an unwrapping process, and hence many phase unwrapping algorithms has been developed specifically for data with a particular application. Moreover, there is no universal phase unwrapping algorithm that can solve wrapped phase data from any application. Therefore, phase unwrapping algorithms are considered as a trade-off problem between accuracy of solution and computational requirements. However, even the most robust and complete phase unwrapping algorithm cannot guarantee in giving successful or acceptable unwrapped results without a good set of initial parameters. Unfortunately, there is no standard or technique to define the parameters that guarantee a good performance on phase unwrapping.

To face the phase unwrapping problems, algorithms can be divided in two categories: local and global phase unwrapping. Local phase unwrapping algorithms find the unwrapped phase values by integrating the phase along a certain path. This is called path-following algorithms [6].

Global phase unwrapping algorithms locate the unwrapped phase by minimizing a global error function and are also called local phase unwrapping algorithm and a global phase unwrapping algorithm, by following the methodology proposed by Pedraza in [1]. The unwrapped phase values and the wrapped phase can be related with each other as:

$$\Psi(n) = \varphi(\pi) + 2\pi k(n) \quad -\pi < \Psi(n) \leq \pi \tag{22}$$

$$\varphi(n) = \Psi(n) + 2\pi v(n) \quad -\infty < \varphi(n) \leq \infty \tag{23}$$

here Ψ(n) holds the wrapped phase values and φ(n) holds the unwrapped phase values, k(n) is the function containing the integers that must be added to the wrapped phase φ to be unwrapped, n is an integer and v(n) is the function containing a set of integers that must be added to the wrapped phase Ψ.

Noting that;

$$v(n) = -k(n) \tag{24}$$

The wrapping operation ω which converts the unwrapped phase is defined by:

$$\varpi\{\varphi(n)\} = \arctan\left[\frac{\sin(\varphi(n))}{\cos(\varphi(n))}\right] \tag{25}$$

3.1 Local Phase unwrapping

Local phase unwrapping algorithms finds the unwrapped phase values by integrating the phase along certain path that covers the whole wrapped phase map. The local phase unwrapping defines the quality of each pixel in the phase map to unwrap the highest quality pixels first and the lowest quality pixels last (quality-guided phase unwrapping). For this purpose, the methods known as residue-balancing are proposed, which attempts to prevent error propagation by identifying residues (the source of noise in the wrapped phase). The residues must be balanced and isolated by using barriers (branch-cuts), therefore, it aims to produce a path-independent wrapped phase map. Path-dependency occurs to the existence of residues.

Residue-balancing algorithms search for residues in a wrapped-phase map and attempt to balance positive and negative residues by placing cut lines between them to prevent the unwrapping path breaking the mesh created. The residue is identified for each pixel in the phase map by estimating the wrapped gradients in a 2 × 2 closed loop, as shown in Figure 2.

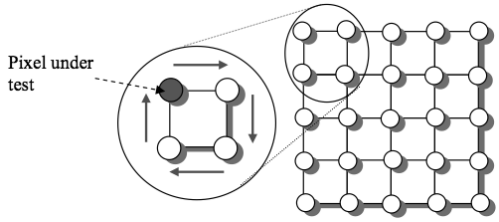

Figure 2. Identifying residues in a 2 × 2 closed path.

This is carried out using the following equation:

$$r = \Re\left[\frac{\Psi_{i,j} - \Psi_{i+1,j}}{2\pi}\right] + \Re\left[\frac{\Psi_{i+1,j} - \Psi_{i+1,j+1}}{2\pi}\right] + \Re\left[\frac{\Psi_{i,j+1} - \Psi_{i,j}}{2\pi}\right] \tag{26}$$

Where $\Re[]$ rounds its argument to the nearest integer, $\Psi_{x,y}$ is the wrapped pixel. The equation 13 can only take three possible results: 0, +1, and -1. A pixel under test is considered to be a positive residue if the value of r is +1, and it is considered to be a negative residue if the value is -1. Conversely, the pixel is not a residue if the value of r is zero. After identifying all residues in the wrapped phase map, these residues have to be balanced by means of branch cuts. Branch-cuts act as barriers to prevent the unwrapping path going thorough them. If these branch cuts are avoided during the unwrapping process, no errors propagate and the unwrapping path is considered to be path independent. On the other hand, if these branch cuts are penetrated during the unwrapping, errors propagate throughout the whole phase map, and in this case the unwrapping path is considered to be path dependent.

3.2 Global phase unwrapping

In the previous section, it was stated that local phase unwrapping algorithms follow a certain unwrapping path in order to unwrap the phase. They begin at a grid point and integrate the wrapped phase differences over that path, which ultimately covers the entire phase map. Local phase unwrapping algorithms (residue-balancing algorithms) generate branch cuts and define the unwrapping path around these cuts in order to minimize error propagation.
In contrast, global phase unwrapping algorithms formulate the phase unwrapping problem in a generalized minimum-norm sense [6]. Global phase unwrapping algorithms attempt to find the unwrapped phase by minimizing the global error function as shown in equation 14

$$\varepsilon^2 = ||\, solution - problem \,||^2 \tag{27}$$

Global phase unwrapping algorithms seek the unwrapped phase whose local gradients in the *x* and *y* direction match, as closely as possible.

$$\varepsilon^2 = \sum_{i=0}^{M-2}\sum_{j=0}^{N-1}\left|\Delta^x\varphi(i,j) - \hat{\Delta}^x\psi(i,j)\right|^p + \sum_{i=0}^{M-1}\sum_{j=0}^{N-2}\left|\Delta^y\varphi(i,j) - \hat{\Delta}^y\psi(i,j)\right|^p \tag{28}$$

Where $\Delta^x\varphi(i,j)$ and $\Delta^y\varphi(i,j)$ are unwrapped phase gradients in the *x* and *y* directions respectively, which are given by:

$$\Delta^x\varphi(i,j) = \varphi(i+1,j) - \varphi(i,j) \tag{29}$$

$$\Delta^y\varphi(i,j) = \varphi(i,j+1) - \varphi(i,j) \tag{30}$$

$\hat{\Delta}^x\psi(i,j)$ and $\hat{\Delta}^y\psi(i,j)$ are the wrapped values of the phase gradients in the *x* and *y* directions respectively, and they are given by:

$$\hat{\Delta}^x\psi(i,j) = \omega\{\psi(i+1,j) - \psi(i,j)\} \tag{31}$$

$$\hat{\Delta}^y\psi(i,j) = \omega\{\psi(i,j+1) - \psi(i,j)\} \tag{32}$$

Finally the wrapping operator is defined by the equation 25.

4 Setup and proposed Methodology

Considering Figure 3, we have a fringe which is projected from the projector, the fringe reaches the object at point H and will cross the reference plane at the point C. By observation, the triangles DpHDc and CHF are similar and since:

$$\frac{CD}{-h} = \frac{d_0}{l_0} \tag{33}$$

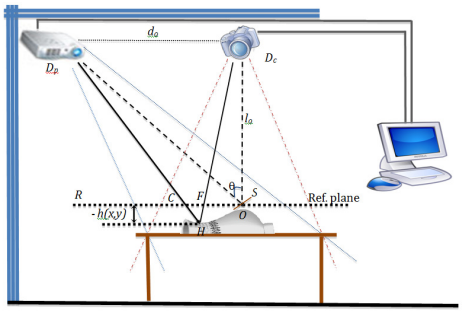

Figure 3. Experimental setup.

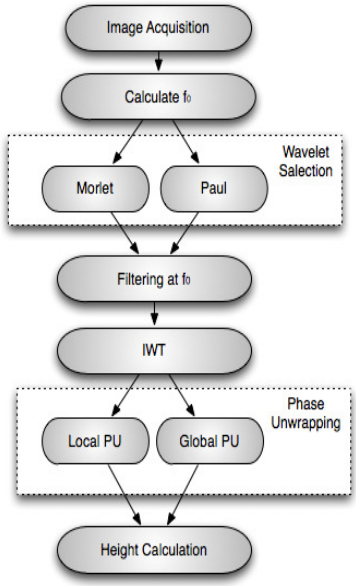

Figure 4. Proposed methodology.

The experimental setup shown in Figure 3 is proposed and during the experiments the methodology in Figure 3 is applied. The first step is to acquire the image. Due to the nature of the image, sometimes a filtering to eliminate the noise is necessary, and a filter is used. Next, the fundamental frequency *fo* is estimated. Later, the mother is selected (Morlet or Paul) and applied. The filter at *fo* is carried out and the Inverse Wavelet transformation is done. At this stage, the information of the height is phase wrapped and two phase unwrapping algorithms are proposed: Local and Global Analysis Algorithm and Graph Cuts Algorithm. The final step is to obtain the object reconstruction and in some cases to determine the error (in case of virtual created objects). The experimental setup uses a high-resolution digital CCD camera and a high resolution digital projector.

The object of interest can be any three-dimensional object and for this work, three objects are considered, which are shown on figure 5.

It is also important to develop software able to produce several different fringe patterns. To create several patterns, it is necessary to modify the spatial frequency (number of fringes per unit area), and resolution (number of levels to create the sinusoidal pattern) of the fringe pattern. It may also be necessary to include into the software development a routine capable of performing phase shifting as well as to include the horizontal or vertical orientation projection of the fringe pattern.

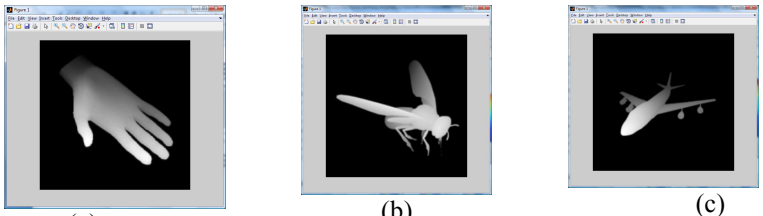

(a) (b) (c)

Figure 5. Virtual objects used in the test: (a) Hand, (b) Fly, and (c) Airplane.

5 Results

To test the methodology, first an object with Hand shape is used. Then, a sinusoidal fringe pattern of known spatial frequency is created with 128 fringes and added to the shape of the created object. The resulting image is shown in Figure 6(c). It is worth noting the distortions of the fringe pattern due to the object´s shape.

The wrapped phase and its mesh are shown in Figure 6. The reconstructed Hand using the Morlet Wavelet Transform and applying the Local PU Analysis and the Global PU Analysis can be seen in Figure 7. Notice that, by applying this method, the shape of the Hand looks almost equal, but it has an error magnitude of about 3.2 and 2.1% respectively.

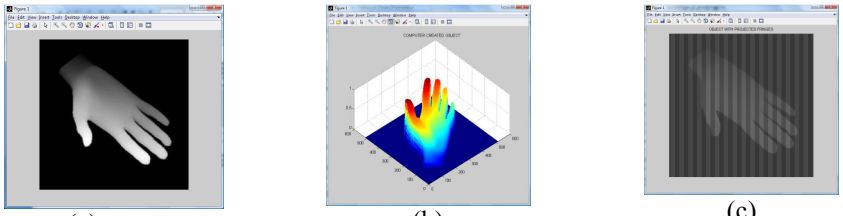

(a) (b) (c)

Figure 6. Computer created Hand: (a) Object image, (b) Object mesh, and (c) fringes projected on it.

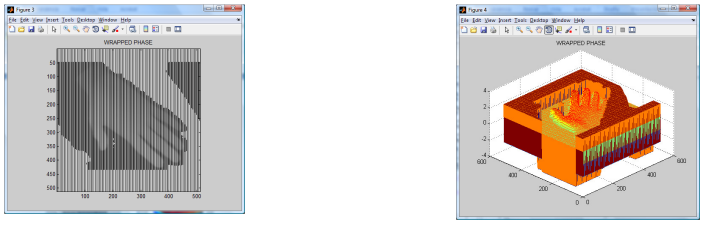

Figure 7. Wrapped phase (image and mesh).

(a) (b)

Figure 8. Reconstructed object using Morlet Wavelet and (a) Local Phase Unwrapping Algorithm, and (b) Global Phase Unwrapping Algorithm.

The results on Figure 8 show that the whole volume presents an acceptable error and the shape is well defined. The mother wavelet used was the Morlet but the same experiment was conducted for the Paul wavelet ant the results are presented on. The computer simulation allowed us to test and proposed methodology.

To validate the whole methodology, more experiments were conducted considering the objects observed on Figure 5. Those objects have different shapes (computer created), where the height is known in every point in the object. Then, the Morlet and Paul mother Wavelets are considered as well as the two different phase unwrapping algorithms. As a second experiment, Paul Wavelet is used and height of the virtual object was compared with each one of the analysis and the results are presented in figure 9.

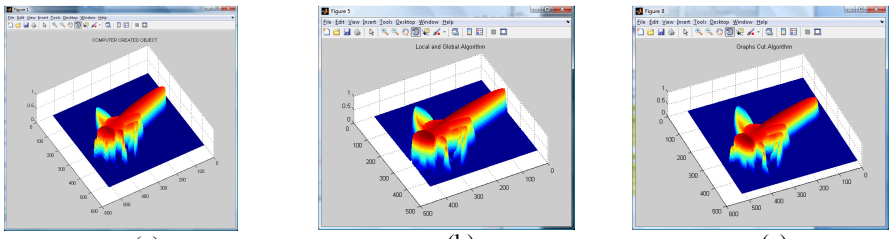

(a) (b) (c)

Figure 9. Fly object and its reconstruction using Paul Wavelet: (a) Object, (b) Local PU Algorithm, and (c) Global PU Algorithm.

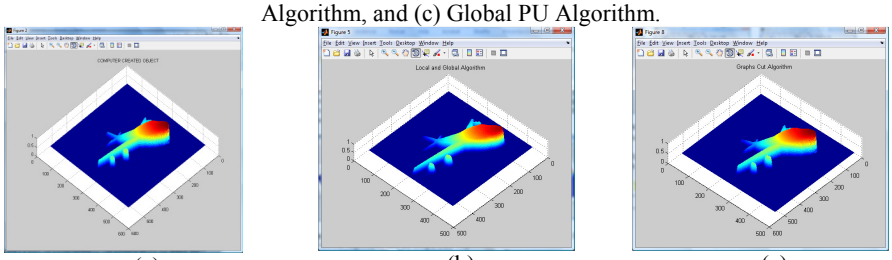

(a) (b) (c)

Figure 10. Airplane object and reconstruction using Morlet Wavelet: (a) Object, (b) Local PU Algorithm, and (c) Global PU Algorithm.

Third experiment was conducted with Morlet Wavelet and the object used was the airplane, and the respective results of the reconstruction process can be seen in Figure 10. Later, all the experiments are joined and the error magnitude is enclosed on tables

1 and 2. The results show that the better performance was obtained by using the Morlet wavelet together with the Global Phase Unwrapping Algorithm in final step to do the 3D reconstruction process.

Table 1. Error table using Morlet Wavelet.

Object	Local and Global	Graph Cuts
Hand	3.26	2.11
Fly	3.47	2.21
Airplane	3.51	2.18

Table 2. Error table using Paul Wavelet.

Object	Local and Global	Graph Cuts
Hand	4.37	3.43
Fly	4.65	3.76
Airplane	4.71	3.55

Finally, the performance of the proposed methodology was tested in a real object (Volleyball) and both Morlet and Paul wavelets were used considering the Global Phase Unwrapping Algorithm for the phase unwrapping and the results can be observed in Figure 11.

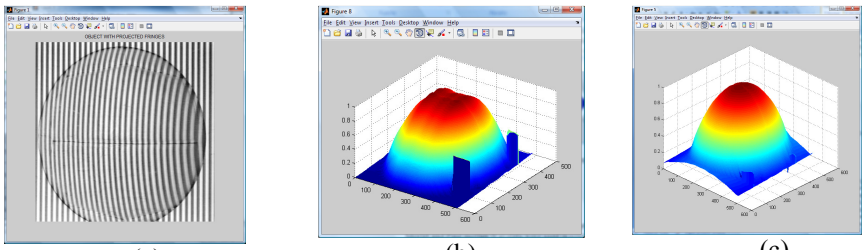

(a) (b) (c)

Figure 11. Real object and reconstruction: (a) Object, (b) Using Morlet Wavelet, and (c) Paul Wavelet with Graph Cuts Algorithm.

6 Conclusions and Future Work

In this work, an enhanced Wavelet based Profilometry was presented and tested. Both Morlet and Paul mother Wavelets were used in conjunction with Local and Global techniques, as well as Graph Cuts Algorithms in the phase unwrapping process. Three different objects generated by the computer were utilized (Hand, Fly and Airplane). The object's projected fringe pattern has a known spatial frequency. Also, a real object was chosen and the methodology was carried out with an accurate reconstruction of the object. Among the proposed wavelets, the one who shows a better performance was the Morlet wavelet in comparison with Paul wavelet, because

Morlet was the one that produced a minimal error. As a conclusion, we can say that the proposed methodology could be used to digitize diverse objects with good results. As a future work, the software performance can be improved in order to implement it inside an embedded system.

References

1. Gokstorp, M. Depth Computation in Robot Vision; Ph.D. Thesis, Department of Electrical Engineering, Linkoping University: Linkoping, Sweden, 1995.
2. Takeda, M.; Ina, H.; Kobayashi, S. Fourier-Transform method of fringe pattern analysis for computed-based topography and interferometry. J. Opt. Soc. Am. 1982, 72, 156-160.
3. Grevenkamp, J.E.; Bruning, J.H. Phase-shifting interferometry. In Optical Shop Testing; Malacara, D. Ed.; Wiley: New York, NY, USA, 1992.
4. K. Creath, in: W.R. Robinson, G.T. Reid (Eds.), Interferogram Analysis: Digital Fringe Pattern Measurement Techniques, Institute of Physics, Philadelphia, PA, 1993.
5. M. Gdeisat, D. Burton, M. Lalor, Appl. Opt. 39 (2000) 5326.
6. Y. Ichioka, M. Inuiya, Appl. Opt. 11 (1972) 1507.
7. Berryman, F.; Pynsent, P.; Cubillo, J. A theoretical Comparison of three fringe analysis methods for determining the three-dimensional shape of an object in the presence of noise. Opt. Lasers Eng. 2003, 39, 35-50,
8. Pedraza, J.C. et al, Image Processing for 3D Reconstruction using a Modified Fourier Transform Profilometry Method; Springer-Verlag: Berlin, Germany, 2007; pp. 705–712.
9. Rastogi, P.K. Digital Speckle Pattern Interferometry and Related Techniques; Wiley: New York, NY, USA, 2001.
10. Itoh, K. Analysis of the phase unwrapping algorithm. Appl. Opt. 1982, 21, 2470-2486.
11. Wu, L.S. Research and development of fringe projection-based methods in 3D shape reconstruction. J. Zhejiang Univ. Sci. A 2006, 7, 1026-1036,
12. Zhong, J.G.; Wang, J.W. Spatial carrier-fringe pattern analysis by means of wavelet transform: wavelet transform profilometry. Appl. Opt. 2004, 43, 4993-4998.
13. Zang, Q.; Chen, W.J.; Tang, Y. Method of choosing the adaptive level of discrete wavelet decomposition to eliminate zero component. Opt. Commun. 2009, 282, 778-785.
14. Dursun, A.; Ozder, S.; Ecevit, N. Continuous wavelet transform analysis of projected fringe pattern analysis. Meas. Sci. Tech. 2004, 15, 1768-1772.
15. Afifi, M. et al, Wavelet-based algorithm for optical phase distribution evaluation. Opt. Commun. 2002, 211, 47-51.
16. Gdeisat, M.A.; Burton, D.R.; Lalor, M.J. Spatial carrier fringe pattern demodulation using a two-dimensional continuous wavelet transform. Appl. Opt. 2006, 45, doi:10.1364/AO.45.008722.
17. Pedraza-Ortega, J.C. et al, Three-Dimensional Reconstruction System based on a Segmentation Algorithms and a Modified Fourier Transform Profilometry. In Proceedings of the IEEE Electronics, Robotics and Automotive Mechanics Conference, Cuernavaca, Morelos, September, 2009.
18. Pedraza-Ortega, J.C. et al, A Profilometric Approach for 3D Reconstruction Using Fourier and Wavelet Transforms. In MICAI 2009: Advances in Artificial Intelligence; Springer Berlin-Heidelberg: Berlin, Germany, 2009; pp. 313-323.
19. Gdeisat, M.A.; et al, Spatial and Temporal Carrier Fringe Pattern Demodulation using the One-Dimensional Continuous Wavelet Transform: Recent Progress, Challenges and Suggested Developments. Opt. Lasers Eng. 2009, 47, 1348-1361.